electrostatic interactions will decrease upon increase of the distance between the charged group on the ligand and the binding site of CAII. To test this hypothesis, we compared ligands **4**, **5**, and **6**, in which the negatively charged carboxylate group was separated from the sulfonamide group by increasing numbers of bonds (Fig. 2B). The dependence of free energy of binding on charge, $\Delta\Delta G_b/\Delta Z$, for ligands **4**, **5**, and **6** was 0.10 ± 0.01, 0.07 ± 0.02, and 0.02 ± 0.02 kcal mol^{-1} charge^{-1}, respectively. As expected, the interactions between the charges on ligands and proteins decreased as the number of bonds between the sulfonamide group and the charged group increased. The value of $\Delta\Delta G_b/\Delta Z$ for **4** is approximately twice that of the shorter ligand **1**; we have not established the origin of this difference.

Three characteristics of the combination of ACE and charge ladders are particularly useful for study of electrostatic contributions to the free energies of protein-ligand interactions. First, it generates large numbers of directly comparable data in a straightforward experimental system. Second, charge ladders can be generated from a large number of proteins, and although only certain charge ladders behave as simply as that from CAII, the technique has useful generality (*19*). Third, the technique readily permits quantitative evaluation of both intensive (ion composition and temperature) and extensive (ionic strength and pH) influences on the electrostatic contribution to biological interactions.

REFERENCES AND NOTES

1. B. Honig and A. Nicholls, *Science* **268**, 1144 (1995).
2. K. J. Lumb and P. S. Kim, *ibid.*, p. 436.
3. J. Novotny and K. Sharp, *Prog. Biophys. Mol. Biol.* **58**, 203 (1992).
4. The observation that interactions between colloidal particles of like charge can, in certain instances, be attractive further complicates our understanding of electrostatic effects in ionic media [N. Ise and H. Yoshida, *Acc. Chem. Res.* **29**, 3 (1996); K. S. Schmitz, *ibid.*, p. 7].
5. P. G. Thomas, A. G. Russell, A. J. Fersht, *Nature* **318**, 375 (1985).
6. J. Gao, F. A. Gomez, R. Haerter, G. M. Whitesides, *Proc. Natl. Acad. Sci. U.S.A.* **91**, 12027 (1994).
7. S. J. Dodgson, R. E. Tashian, G. Gros, N. D. Carter, Eds., *The Carbonic Anhydrases: Cellular Physiology and Molecular Genetics* (Plenum, New York, 1991).
8. Y.-H. Chu, L. Z. Avila, J. Gao, G. M. Whitesides, *Acc. Chem. Res.* **28**, 461 (1995).
9. S. K. Basak and M. R. Ladisch, *Anal. Biochem.* **226**, 51 (1995).
10. H. A. Abramson, L. S. Moyer, M. H. Gorin, *Electrophoresis of Proteins and the Chemistry of Cell Surfaces* (Reinhold, New York, 1942), chaps. 5 and 6.
11. The charge ladder of CAII was prepared as follows. The pH of three solutions of native CAII (0.1 mM in distilled water, 0.5 ml) was adjusted to pH 10 by addition of 0.1 N NaOH and was maintained at this value. Acetic anhydride (10, 20, and 40 equiv, respectively, 100 mM in dioxane) was added. After 30 min, the three solutions were mixed and diluted to 10 μM in a buffer of 25 mM tris and 192 mM Gly (pH = 8.3). This procedure gave a sample in which each member of the charge ladder could be easily analyzed. The neutral marker was 4-methoxybenzyl alcohol (50 μM).
12. We used a Beckman P/ACE 5500 system for CE. General conditions: operated at 15 kV; temperature T = 37°C, maintained by liquid cooling; capillary inner diameter, 50 μm; total length of capillary, 47 cm; length from inlet to detector, 40 cm. For the ACE experiments, different concentrations of a ligand were prepared in a buffer of 25 mM tris and 192 mM Gly (pH = 8.3). The capillary was flushed with 0.1 N NaOH, distilled water, and electrophoresis buffer for 2 min before each experiment.
13. Using competitive ACE (*8*), we measured the binding affinities of the neutral ligands **2** and **3** to CAII by competition with ligand **1** (+1 charge), and that of neutral ligand **7** by competition with ligand **5** (−1 charge).
14. A conventional fluorescence assay on samples containing mixtures enriched in low-Z_n and high-Z_n fractions of the charge ladder of CAII confirmed qualitatively the influence of its charge, and that of its ligands, on ΔG_b.
15. The lines that correlate ΔG_b with Z_n in Fig. 2 can be extrapolated to Z_n = 0. At this point, the influence of charge-charge interactions on binding should disappear. For ligands with the same structure inside the active site (Fig. 2B), the lines can be extrapolated to a common point (ΔG_b = −8.4 ± 0.1 kcal mol^{-1}) at Z_n = 0; for ligands with different structure inside the active site (Fig. 2A), the lines do not intersect at Z_n = 0, and therefore, other factors (for example, pK_a of sulfonamide groups or hydrophobic interactions) must contribute to differences in binding.
16. The dimensions of CAII taken from its crystal structure are 41 Å by 41 Å by 47 Å [A. Liljas *et al.*, *Nature* **235**, 131 (1972)].
17. We attribute the nonintegral net charge for CAII (Z_0 = −3.5) at pH 8.3 to the fractional protonation of charged residues such as His or water bound to Zn(II).
18. Dissolved salts should lower this calculated electrostatic cost further by partially screening the charges on CAII from those on ligands.
19. We have observed similar electrostatic effects on binding in three other systems. One comprises a monoclonal antibody, rat immunoglobulin IgG2b, interacting with differently charged synthetic ligands (ligand charges Z_L = −1, −3, −6, and −9) that contain a dinitrophenyl group. The observed free energy of binding correlated linearly with the charge on the ligand: $\Delta\Delta G_b/\Delta Z$ = 0.030 ± 0.006 kcal mol^{-1} charge^{-1}. The second system comprises vancomycin interacting with D-Ala–D-Ala; the observed value of $\Delta\Delta G_b/\Delta Z$ was 1.2 kcal mol^{-1} charge^{-1}. This larger value of electrostatic effect is consistent with a shorter distance between the two charged groups on vancomycin and the carboxylate group of D-Ala–D-Ala. The third system comprises a charge ladder of carboxypeptidase B interacting with Arg; the observed value of $\Delta\Delta G_b/\Delta Z$ was 0.05 ± 0.02 kcal mol^{-1} charge^{-1}. In all three systems, opposite charges stabilized the receptor-ligand complexes and like charges destabilized them. A number of proteins—including lysozyme, superoxide dismutase, peroxidase, dextranase, carboxypeptidase A, ribonuclease A, and papain—produce useful charge ladders on acetylation; we are using these ladders to examine electrostatic influences on binding their substrates or ligands.

20. This work was supported by NIH grant GM 51559. We thank J. Rao for helpful discussions and for the data involving vancomycin.

8 December 1995; accepted 12 March 1996

Adaptive Evolution of Human Immunodeficiency Virus–Type 1 During the Natural Course of Infection

Steven M. Wolinsky,*† Bette T. M. Korber,† Avidan U. Neumann, Michael Daniels, Kevin J. Kunstman, Amy J. Whetsell, Manohar R. Furtado, Yunzhen Cao, David D. Ho, Jeffrey T. Safrit, Richard A. Koup

The rate of progression to disease varies considerably among individuals infected with human immunodeficiency virus–type 1 (HIV-1). Analyses of semiannual blood samples obtained from six infected men showed that a rapid rate of CD4 T cell loss was associated with relative evolutionary stasis of the HIV-1 quasispecies virus population. More moderate rates of CD4 T cell loss correlated with genetic evolution within three of four subjects. Consistent with selection by the immune constraints of these subjects, amino acid changes were apparent within the appropriate epitopes of human leukocyte antigen class I–restricted cytotoxic T lymphocytes. Thus, the evolutionary dynamics exhibited by the HIV-1 quasispecies virus populations under natural selection are compatible with adaptive evolution.

In general, the natural history of HIV-1 infection in humans follows a defined pattern with well-characterized features (*1*–*3*); however, the rates of development of disease and the survival times in different individuals vary widely (*4*). The pathogenic potential of the virus (*5*–*8*) and the immunopathogenic effects of the immune response (*9*) have each been postulated to explain the observed differences in progression to disease. One hypothesis that might explain the variable course is that the loss of CD4 T cells in HIV-1–infected individuals is primarily due to increasing antigenic diversity that, beyond a threshold, exceeds the capacity of the immune response to regulate viral population growth (*10*).

To evaluate this hypothesis critically, we directly measured the levels of HIV-1 RNA and tracked viral sequence changes that occurred in concert with the humoral and cellular immune response in samples from a well-defined cohort of HIV-1–infected individuals. Six men with confirmed HIV-1

infection from the Chicago component of the Multicenter AIDS Cohort Studies (MACS) were selected on the basis of differences in their rates of CD4 T cell count decline at ~6-month-interval study visits (Table 1). Two subjects each had a rapid (P1 and P2) or moderate (P3 and P4) rate of CD4 T cell loss, and two had a relatively stable CD4 T cell count (P5 and P6). The depletion rate for the CD4 T cell subset correlated with the plasma HIV-1 virion–associated RNA burden ~9 months after primary infection, a time when this value generally stabilized, and with the ratio of intracellular unspliced and multiply spliced mRNAs (Table 1). The average HIV-1 virion–associated RNA burden over the subsequent follow-up period also correlated with these values (Table 1).

To explore the relation between disease progression and genetic diversity, we tracked the evolution of viral sequences within these individuals by examining proviral sequences spanning V3 through V5 amplified by the polymerase chain reaction (PCR) from blood samples obtained during interval visits (*8*). Product DNAs from five to eight time points per individual were cloned, and up to 13 clones from each sample were sequenced (*11*), for a total of 292 sequences, each 650 nucleotides in length.

Phylogenetic analyses of these sequences [(*12*); but see (*13*)] revealed distinct clusters of viral sequences for each subject, indicative of absence of PCR-product contamination. Greater branch lengths were observed for subjects P3, P4, and P5 relative to those for P1, P2, and P6. This observation held when viral sequences were analyzed from comparable time points relative to the time of primary infection (*14*). Thus, the longer branches for subjects P3, P4, and P5 were due to a more rapid accumulation of mutations and not to a longer survival time.

Within each subject, viral diversification and evolution were tracked over time. Viral sequences from P1 and P2 showed no tendency to form clusters associated with sampling time in the phylogenetic reconstructions. Viral sequences from subject P3, in contrast, showed distinctive clustering with sampling time (Fig. 1A). Viral sequences from P4, P5, and P6 had some tendency to cluster with time, with early sequences clustering closer to the ancestral

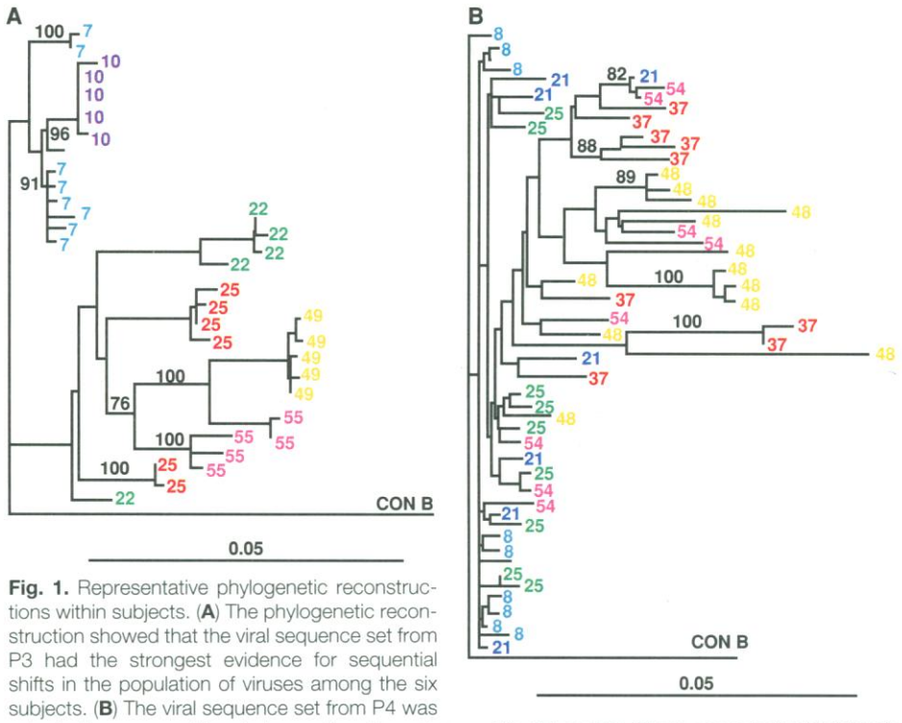

Fig. 1. Representative phylogenetic reconstructions within subjects. (**A**) The phylogenetic reconstruction showed that the viral sequence set from P3 had the strongest evidence for sequential shifts in the population of viruses among the six subjects. (**B**) The viral sequence set from P4 was selected to represent the phylogenetic pattern observed for P4 and P5. There was substantial intermingling of viral sequences from different time points, with generally low bootstrap values representing different clusters. The phylogenetic reconstructions shown are neighbor-joining trees with bootstrap proportions of greater than 75 of 100 bootstrap replicates (shown at appropriate branch points). The PHYLIP program (*40*) was used to construct the tree by means of a Kimura two-parameter distance matrix with a ratio of transition to transversion of 1.3. The B clade consensus sequence (*39*), defined as the most common nucleotide in a given position, was used as an out group. Qualitatively similar trees were generated by means of the maximum likelihood program, in PHYLIP, dnaml. Comparable bootstrap values were also obtained for the nodes in P3 by means of parsimony and the program PAUP (*12, 41*). The taxa are labeled by a number indicating months from the estimated time of primary infection, with each time point represented by a different color. Some outliers and some intermingling of sequences from sequential time points were observed, even in P3, and would be expected, given that the CD4 T cell population can serve as a reservoir of unexpressed provirus.

node at the base of the phylogenetic tree (Fig. 1B). Therefore, progressive shifts in the viral population may be occurring in subjects who have a relatively slow rate of CD4 T cell decline (*15*), as illustrated by P3 and to a lesser extent by P4 and P5.

To test whether the observed difference in the evolutionary rates within subjects was due to positive selection or to differences in replication kinetics, we compared the accumulation rates of nonsynonymous relative to synonymous base substitutions in all sequences by using the consensus sequence of the first time point as a reference (*16*). The accumulation rates of nonsynonymous substitutions were faster in subjects P3, P4, and P5 (1.5, 1.0, and 1.3% per annum, respectively) than in P1 and P2 (0.5 and 0.3% per annum, respectively). The slower accumulation rate of nonsynonymous substitutions for P6 (0.3% per annum) was an exception to the trend. In contrast, the rates of accumulation of synonymous base substitutions were gradual and comparable in all subjects (0.3 to 0.5% per annum), with the exception of P2, who had fewer changes (*17*). Therefore, within the limitations of our data set ($n = 6$), the increase in genetic diversity correlated with positive selection for change and, contrary to prediction (*10*), with prolonged rather than shortened survival (*18*).

To determine whether an antigenic diversity threshold existed for each of these six subjects (*10*), and to facilitate tracking viral forms through time, we devised a method for systematically clustering closely related protein sequences that could be regarded as predictive of immunological reactivity (*19*). Because of the relatively long length of the viral sequences analyzed in this study, it was not possible to define genetic forms on the basis of sequence identity as was done previously when only the 35 amino acids of the V3 loop were considered (*10*). Therefore, to estimate viral diversity in a sample and explore shifts in the HIV-1 quasispecies virus population, we generated pairwise similarity scores for all aligned protein sequences and clustered the scores by using phenograms that group sequences according to

S. M. Wolinsky, M. Daniels, K. J. Kunstman, A. J. Whetsell, M. R. Furtado, Department of Medicine, Northwestern University Medical School, 303 East Chicago Avenue, Chicago, IL 60611, USA.
B. T. M. Korber and A. U. Neumann, Theoretical Division, T-10, Los Alamos National Laboratory, Los Alamos, NM 87545, USA.
Y. Cao, D. D. Ho, J. T. Safrit, R. A. Koup, The Aaron Diamond AIDS Research Center and The Rockefeller University, 455 First Avenue, New York, NY 10016, USA.
*To whom correspondence should be addressed.
†These two authors contributed equally to the conceptualization, design, and execution of this work.

Table 1. The clinical course, CD4 T cell depletion rates, and quantitative virological data for the six study subjects. The times of infection, estimated as the midpoint between the last HIV-1 antibody negative and the first antibody positive visit, were, for the six subjects, 1984 for P5; 1985 for P1, P2, and P6; and 1986 for P3 and P4. Subjects P2, P3, and P4 received antiretroviral therapy with zidovudine at 30 months, 48 months, and 64 months after the estimated time of infection, respectively. Subject P5 was lost to follow-up after 48 months. P1 and P2 died within 36 and 42 months of infection, respectively. CD4 T cell counts, expressed as numbers of cells per microliter, were determined as described (*38*). The rates of linear CD4 T cell decline were measured by the minimal slope obtained from sliding linear regressions starting within a year after primary infection. Plasma HIV-1 RNA levels were measured by a quantitative RT-PCR assay (Roche Molecular Systems) and expressed as RNA copies per milliliter. Intracellular unspliced and multiply spliced viral mRNAs were measured as described (*8*). Because of the 3- to 6-month sampling intervals, the initial rise and subsequent fall in the plasma viral RNA burden during primary infection was detected only for subjects P2 and P5.

Subject	Follow-up time (months)	CD4 depletion rate		Average CD4/CD8 ratio	Average viral RNA in plasma (copies/ml)	Viral RNA at 9 months after primary infection				Viral RNA at last visit			
		Linear (cells μl^{-1} $month^{-1}$)	Exponential (cells μl^{-1} $month^{-1}$)			Plasma	Unspliced	Spliced	Ratio	Plasma	Unspliced	Spliced	Ratio
P1	32	−19.5	−0.08	0.39	417,338	267,612	6240	1224	5.1	294,745	22,172	2132	10.4
P2	35	−20.5	−0.05	0.21	172,141	120,885	3526	1037	3.4	300,952	22,564	2097	11.1
P3	122	−4.0	−0.013	0.37	49,171	32,444	4121	2264	1.8	28,317	14,282	1359	6.8
P4	116	−3.4	−0.003	0.39	13,367	13,413	987	1974	0.5	8,611	1,237	1359	0.9
P5	47	−0.4	−0.0004	0.53	6,120	10,283	2624	4686	0.6	1,905	16,213	3753	4.3
P6	93	−0.3	−0.0004	0.93	7,923	11,355	750	1250	0.6	3,489	3,216	1524	2.1

amino acid similarity (*19*), irrespective of evolutionary path (*20*). The frequencies of sequences representing different clusters were then used as a basis for calculating the entropy of that sample, where entropy is a measure of variability based on the distribution of discrete forms within a sample (*21*).

All six subjects had relatively homogeneous virus populations up to 9 months after primary infection, showing either one or two protein forms (Fig. 2). Subjects P1 and P2 who progressed rapidly to acquired immunodeficiency syndrome (AIDS) maintained a relatively homogeneous population of protein variants throughout the entire course of infection even at the beginning of a precipitous decline in the CD4 T cell count (Fig. 2) (*15*, *18*, *22*). In contrast, late time points in P4 and P5, when the CD4 T cell count was relatively stable, showed the highest diversity among all the samples (Fig. 2). Subject P3 consistently showed relatively homogeneous within-sample viral sequences, however, even in a period of CD4 T cell decline (Figs. 1 and 2). The progressive changes apparent in P3 (Fig. 2) over time were also seen in the phylogenetic topology (Fig. 1A).

Lacking evidence for increasing antigenic diversity as the driving force behind the rate of CD4 T cell loss (*10*), we assessed the role of the immune response by studying aspects of the humoral and cell-mediated immune surveillance mechanisms. In neutralizing antibody assays performed with both autologous and heterologous primary viruses (*7*), most of the sera obtained from these participants early after infection had little or no neutralizing activity, whereas late in the course of infection, the neutralizing antibody response tended to be more pronounced in the sera obtained from P3, P4, and P6 compared with sera from P1, P2, and P5 (*23*). Contrary to what has been observed in simian immunodeficiency virus infection of macaques (*24*), we found no clear association between the humoral immune response and the rate of progression to AIDS. In contrast, *gag*-, *pol*-, and *env*-specific cytotoxic T lymphocytes (CTLs) were detectable for each of these subjects (*2*), with the frequency of CTL precursors (CTLp) inversely correlated with the rate of progression to disease (Table 2). Two human leukocyte antigen (HLA) class I–restricted CTL epitopes unambiguously defined within the region of gp120 that was sequenced (*25*) also showed a high frequency of amino acid substitutions over time when the subject expressed the given allele and when there was an *env*-specific CTL

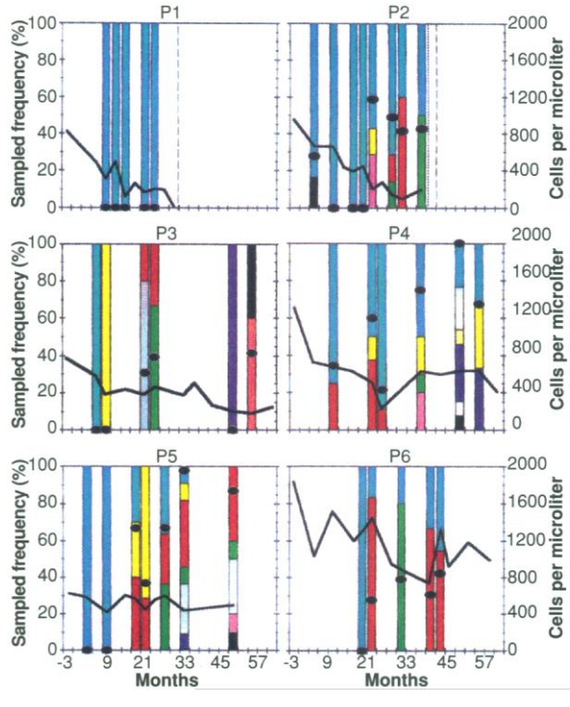

Fig. 2. Diversity of viral forms and shifts in the HIV-1 quasispecies virus populations over time. The STR amino acid substitution matrix, based on the amino acid substitution frequencies found in protein structure–based alignments (*42*), was used for calculating the sequence similarity. Gap penalties were scored such that the initial gap caused a reduction in the total score of 6.7, and additional, consecutive gaps reduced the score by 1.3. Once all pairwise scores were calculated, the viral sequences were clustered by means of maximum linkage (*13*). Sequences were grouped according to the clustering pattern into sets containing highly related forms, with the same criteria used for all six subjects, and represented as histograms (alignments of viral sequences are available upon request). The predominant viral form found in each subject in the first time point is indicated in turquoise. Other forms are indicated by additional colors, with no relation implied between the subsequent colors and the forms found in the different subjects. The fraction of the total number of viral sequences that were of a given form within each sample is shown. To normalize these data and allow for an appropriate scale on the abscissa, the entropy of each sample (*16*) (●) is displayed as a percentage of the highest entropy in the study (P4 sampled at 48 months after infection; entropy = 1.68). Two additional measures of viral variation within samples were calculated: the Simpson index (*10*) and the mean and median Hamming distance for the amino acid sequences, excluding gaps. Both of these distance measurements provided intersubject comparisons that essentially tracked with the entropy measure shown here. CD4 counts (black line) are shown as cells per microliter.

response (Table 2) (*26*). Thus, a vigorous HIV-1–specific HLA class I–restricted CTL response was associated with slow rather than rapid rates of development of disease, contrary to the prediction that the immunopathogenic effects of CTLs are responsible for depletion of CD4 T cells (*9*).

To assess the contribution of viral virulence in mediating CD4 T cell decline in these individuals (*5*, *6*), we examined the biological phenotype of viruses isolated from blood samples obtained from each subject at serial time points (*27*). All viruses replicated with equal efficiency in primary cultures of normal donor peripheral blood mononuclear cells and monocyte-derived macrophages and did not induce syncytia in cultures of the established MT-2–transformed T cell line. Therefore, there was no evidence of a phenotypic switch to syncytium-inducing forms in the virus populations coincident with an accelerated rate of progress to AIDS (*5*). Consistent with these results, the characteristic positively charged amino acids in the V3 loop motif associated with a syncytium-inducing phenotype were absent from all 292 sequences (*28*).

To screen for a potential difference in the ability of these isolated viruses to replicate and deplete CD4 T cells in the absence of any immune response, we inoculated longitudinal viruses isolated from all six study participants into human fetal thymus–re-

B7-restricted epitope *RP*NNNTRKS*I*			Cw4-restricted epitope S*F*NCGGEF*F*			CTLp/10^4 PBMCs *env*	*gag*	*pol*
P1.-3	NA		P1.-3	NA				
P1.9	----------	11	P1.9	---------	10	0.1	0.2	0.7
			P1.9	-------X-	1	1.2	2.6	2.5
P1.13	----------	7	P1.13	---------	8			
P1.13	------G---	1						
P1.16	----------	8	P1.16	---------	8			
P1.22	----------	8	P1.22	---------	7			
			P1.22	-------S-	1			
P1.26	----------	7	P1.26	---------	7	0.3	0.3	0.8
P2.3	--------G-	6	P2.3	---------	6			
P2.9	--------G-	6	P2.9	---------	6			
P2.12	NA		P2.12	NA		0.3	<0.1	<0.1
P2.15	--------G-	7	P2.15	---------	7			
P2.18	--------G-	5	P2.18	---------	5			
P2.21	--------G-	7	P2.21	---------	5	0.3	0.1	0.2
			P2.21	-------L-	1			
			P2.21	C--------	1			
P2.27	--------G-	5	P2.27	---------	7	0.4	0.5	0.2
P2.27	--------GT	1						
P2.27	-----A--G-	1						
P2.31	--------G-	4	P2.31	----------	5			
P2.31	------G-G-	1						
P2.35	--------G-	2	P2.35	------G---	1			
			P2.35	----------	1	<0.1	<0.1	<0.1
P3.-3	NA		P3.-3	NA		<0.1	<0.1	<0.1
P3.7	----------	8	P3.7	---------	8	<0.1	<0.1	<0.1
P3.10	----------	6	P3.10	---------	6			
P3.22	----------	5	P3.22	-----R---	4			
			P3.22	---------	1			
P3.25	----------	4	P3.25	---------	6			
P3.25	----I-----	2						
P3.49	----------	5	P3.49	---------	5			
P3.55	----------	5	P3.55	-------S-	1	0.3	<0.1	0.8
			P3.55	-X-------	1			
			P3.55	---------	3			
P4.8	----------	11	P4.8	---------	10	5.6	19.0	3.6
P4.8	---------T	1	P4.8	--------S	1			
			P4.8	--I------	1			
P4.21	----------	7	P4.21	---------	7	3.3	6.4	5.5
P4.21	--G----R--	1	P4.21	----R----	1			
P4.25	----------	9	P4.25	---------	9			
P4.37	--G----R--	3	P4.37	---------	9			
P4.37	--H-------	2	P4.37	--------L	1			
P4.37	G-S-------	1						
P4.37	--G-D--R--	1						
P4.37	--G-T--R--	1						
P4.37	--S-------	1						
P4.37	----------	1						
P4.48	--S---K---	4	P4.48	---------	9	1.1	4.7	1.1
P4.48	--S-----G-	3	P4.48	------K--	3			
P4.48	--S-------	2	P4.48	G--------	1			
P4.48	----------	2						
P4.48	--GTT--R--	1						
P4.48	$-S-----GM	1						
P4.54	----------	2	P4.54	---------	6			
P4.54	--G----R--	2						
P4.54	--S-------	1						
P4.54	--S-----G-	1						
P6.17	NA		P6.17	NA		0.1	<0.1	9.4
P6.19	----------	10	P6.19	---------	10			
P6.22	----------	6	P6.22	---------	6			
P6.26	NA		P6.26	NA		0.12	0.1	4.4
P6.29	----------	10	P6.29	---------	9			
			P6.29	---R-----	1			
P6.39	----------	3	P6.39	---------	3			
P6.42	----------	10	P6.42	---------	11			
P6.42	--FY------	1						
P6.58	NA		P6.58	NA		<0.1	0.3	3.4
P5.3	----------	13	P5.3	---------	12	<0.1	14.3	<0.1
			P5.3	------K--	1			
P5.9	----------	9	P5.9	---------	10	<0.1	4.0	26.0
P5.9	------K---	1						
P5.19	----------	10	P5.19	---------	10			
P5.23	----------	7	P5.23	---------	7			
P5.28	----------	11	P5.28	---------	11			
P5.34	----------	8	P5.34	---------	11			
P5.34	--D-------	1						
P5.34	K-----G---	1						
P5.34	--S-------	1						
P5.47	--S-------	6	P5.47	---------	10	2.3	4.3	14.8
P5.47	----------	3						
P5.47	--S-----G-	1						

Table 2. A B7-restricted epitope (*RP*NNNTRKS*I* from amino acid position 303 to 312) and a Cw4-restricted epitope (S*F*NCGGEF*F* from amino acid position 380 to 388) are within the region of gp120 that was sequenced (*25*). The amino acid positions are numbered according to the envelope of the HXB2R sequence in the AIDS and Human Retroviruses Database (*39*). P1 and P2 expressed the Cw4 allele, had low to undetectable CTLp against the vaccinia-expressed *env* protein, and had infrequent nonsynonymous substitutions within this epitope. P4, P5, and P6 expressed the B7 allele. P6 lacked nonsynonymous substitutions in the B7-restricted epitope and had a nondetectable *env*-specific CTLp. P4 and P5 had multiple amino acid substitutions within the B7-restricted epitope at time points when strong *env*-specific CTLp was detected. At the first time point tested, P4 and P5 carried the defined B7-restricted epitope, *RP*NNNTRKS*I*, in 11 of 12 and 13 of 13 sequences, respectively. By 37 months, the initial epitope sequence in P4 was almost entirely replaced (1 of 10 remaining) by a variety of forms, many with multiple substitutions. This diversification persisted at 48 and 54 months after infection. At 47 months after infection when P5 had vigorous *env*-specific CTLp, 3 of 10 sequences had the original epitope and 7 sequences had variant epitopes. For subjects P1, P2, and P3 who did not have the B7 allele and P6 who did not have CTLp, only 6 of 162 sequences had single amino acid substitutions within the defined epitope. No epitopes with multiple amino acid substitutions were observed. The anchor residues, highlighted in italics, were essentially unchanged, suggesting that new T cell receptor rearrangements might be able to respond to the variant epitope sequences. Because it is not possible to predict CTL escape solely on the basis of amino acid sequence information, studies are in progress to test the binding of variant epitope peptides to HLA B7 and the recognition of variant peptide-HLA complexes by CTL from these subjects and others (*26*). NA, not applicable; X, any amino acid; $, stop codon. Abbreviations for the amino acid residues are as follows: C, Cys; E, Glu; F, Phe; G, Gly; I, Ile; N, Asn; P, Pro; R, Arg; S, Ser; and T, Thr.

constituted severe combined immunodeficiency mice (SCID-Hu) (*29*). The viruses from all six subjects, regardless of their course of progression to disease, replicated and depleted CD4 T cells to an equivalent extent in the SCID-Hu mouse model (*30*). Therefore, for these six subjects, the viral phenotype was not an overt determinant of the rate of development of disease (*5, 6*).

Models that relate increasing antigenic diversity (*10*), an immunopathologic effect of CTLs (*9*), or dominance of a viral form with a more cytopathic phenotype (*5*) to pathogenic progression are not supported by the results of this study. Within the limitations of our sampling, increasing viral diversity in itself does not correlate with CD4 T cell loss and progression to AIDS. On the contrary, rapid CD4 T cell decline can and does occur when viral populations appear to be relatively homogeneous (*15, 18, 28*). Furthermore, these data suggest that a rapid decline in the CD4 T cell count can occur when an HIV-1–specific immune response is deficient and a predominant viral form with great pathogenic potential is lacking. The presence of diverse viral forms at a given time point may reflect the length of time after primary infection, or shifts in the viral population possibly related to survival advantage during changes in the host environment [for example, a vigorous cell-mediated immune response (*2, 31*) or a change in cell tropism (*5*)]. These factors may account for previous observations in two subjects that related diversity in the V3 loop of *env* to progression of disease (*10*).

Despite the ability of the virus populations to exhibit extreme rates of evolution under selective constraints, stable viral population equilibrium can be found when the starting virus is relatively fit and replicating in a defined, relatively constant environment (*32–35*). In such a milieu, a particular genetic variant, regardless of its pathogenic potential (*32, 33*), would be amplified preferentially. Conversely, in a changing environment or under selective constraints (*32, 34*), population disequilibrium can be found whereby viral replication results in rapid and continuous genetic variation (*32–38*). This paradigm is supported by the phylogenetic analyses within subjects, which showed a relative evolutionary stasis with little evidence of selective pressure for change in subjects P1 and P2, and rapid evolution with some evidence of selective pressure for change in subjects P3, P4, and P5. The slow evolution exhibited by P6 may represent the apparent predominance of some optimally adapted form (*32–38*). Compatible with this paradigm, it is conceivable that the relative stability of the HIV-1 quasispecies virus population in P6 may eventually be disrupted by new selective pressures (*32*). Thus, these data suggest that HIV-1 quasispecies virus population dynamics are compatible with an ideal Darwinian system (*38*).

REFERENCES AND NOTES

1. E. S. Daar, T. Mougdil, R. D. Meyer, D. D. Ho, *N. Engl. J. Med.* **324**, 961 (1991); C. Graziozi *et al.*, *Proc. Natl. Acad. Sci. U.S.A.* **90**, 6405 (1993); M. S. Saag *et al.*, *J. Exp. Med.* **172**, 1055 (1991); S. J. Clark *et al.*, *N. Engl. J. Med.* **324**, 954 (1991).
2. S. M. Wolinsky *et al.*, *Science* **255**, 1134 (1992); T. Zhu *et al.*, *ibid.* **261**, 1179 (1993); L. Q. Zhang *et al.*, *J. Virol.* **67**, 3345 (1993); N. Ahmed, B. M. Baroudy, R. C. Baker, C. Drappy, *ibid.* **69**, 1001 (1995); J. W. Mellors *et al.*, *Ann. Intern. Med.* **122**, 573 (1995); E. C. Holmes, L. Q. Zang, P. Simmonds, C. A. Ludlam, A. J. Leigh-Brown, *Proc. Natl. Acad. Sci. U.S.A.* **89**, 4835 (1992); B. T. M. Korber *et al.*, *AIDS Res. Hum. Retroviruses* **8**, 1461 (1992); C. L. Kuiken *et al.*, *J. Virol.* **66**, 4622 (1992); T. F. W. Wolfs, G. Zwart, M. Bakker, J. Goudsmit, *Virology* **189**, 103 (1992).
3. R. A. Koup *et al.*, *J. Virol.* **68**, 4640 (1994).
4. M. E. Eyster, J. O. Ballard, M. H. Gail, J. E. Drummond, J. J. Goedert, *Ann. Intern. Med.* **110**, 963 (1989); G. Rutherford *et al.*, *Br. Med. J.* **301**, 1183 (1990); H. Sheppard, W. Lang, M. Ascher, E. Vittinghoff, W. Winklestein, *AIDS* **7**, 1159 (1993); S. Buchbinder, M. Katz, N. Hessol, P. O'Malky, S. Holmberg, *ibid.* **8**, 393 (1994); L. K. Schrager, J. M. Young, M. G. Fowler, B. J. Mathieson, S. H. Vermund, *ibid.*, p. 895; I. Kelt *et al.*, *J. Infect. Dis.* **169**, 1236 (1994); T. C. Greenough *et al.*, *AIDS Res. Hum. Retroviruses* **10**, 395 (1994).
5. B. Asjo *et al.*, *Lancet* **ii**, 660 (1986); M. R. Tersmette *et al.*, *J. Virol.* **62**, 2026 (1988); M. R. Tersmette *et al.*, *ibid.* **63**, 2118 (1989); H. Schuitemaker *et al.*, *ibid.* **66**, 1354 (1992); R. I. Connor, H. Mohri, Y. Cao, D. D. Ho, *ibid.* **67**, 1772 (1993); C. Nielsen, C. Pederson, J. D. Lundgren, J. Gerstoft, *AIDS* **7**, 1035 (1993); M. Koot *et al.*, *Ann. Intern. Med.* **118**, 742 (1993); R. Connor and D. D. Ho, *J. Virol.* **68**, 4400 (1994); D. Richman and S. Bozzette, *J. Infect. Dis.* **169**, 968 (1994).
6. J. Learmont *et al.*, *Lancet* **341**, 113 (1993); R. C. Desrosiers, *AIDS Res. Hum. Retroviruses* **8**, 411 (1992); N. L. Michaels *et al.*, *J. Virol.* **69**, 1868 (1995); N. L. Michaels *et al.*, *ibid.*, p. 6758; F. Kirchhoff, T. C. Greenough, D. B. Brettler, J. L. Sullivan, R. C. Desrosiers, *N. Engl. J. Med.* **332**, 228 (1995); A. K. M. Iversen *et al.*, *J. Virol.* **69**, 5743 (1995).
7. Y. Cao, L. Qin, L. Zhang, J. T. Safrit, D. D. Ho, *N. Engl. J. Med.* **332**, 201 (1995).
8. M. F. Furtado, L. Kingsley, S. M. Wolinsky, *J. Virol.* **69**, 2092 (1994).
9. R. M. Zinkernagel and H. Hengartner, *Immunol. Today* **15**, 262 (1994); R. Cheymier *et al.*, *Cell* **78**, 373 (1994); S. Wain-Hobson, *Nature* **373**, 102 (1995).
10. M. Nowak *et al.*, *Science* **254**, 963 (1991); M. Nowak and A. J. McMichael, *Sci. Am.* **273**, 58 (August 1995).
11. The positions of the oligonucleotide primers are numbered according to the HXB2 isolate in the Human Retroviruses and AIDS Database (*39*). KK1-KK3 [nucleotides (nt) 6094 to 6119, 5′-TAATCAG(T/C)TTATGGGATCAAAGCCT-3′; and nt 7332 to 7357, 5′-GTCCTTCCTGCTGCTCCCAAGAACC-3′] and KK2 Eco RI–KK4 Xba I [nt 6122 to 6147, 5′-GAATTCCCATGTGTAAAATTAACCCCACTCT-3′; and nt 7282 to 7307, 5′-TCTAGATGCTCTTTTTTCTCT(C/T)T(G/C)CACCACT-3′] were the outer and inner sets of amplification primers, respectively. The input DNA molecules were quantified as described (*8*). PCR was performed as described [B. T. M. Korber *et al.*, *J. Virol.* **68**, 7467 (1994)] with a Perkin-Elmer/Cetus 9600 automated thermal cycler programmed for 32 cycles at 98°C for 10 s, 50°C for 15 s, and 72°C for 2 min with a final extension at 72°C for 10 min. A 5-μl sample was reamplified in a 100-μl reaction mix containing 0.2 μM of each of the inner primer pair by means of the same cycle profile as above. HIV-1–negative cell DNA and reagent controls were run in parallel [S. Kwok and R. Higuchi, *Nature* **339**, 237 (1989)]. PCR-product DNA was asymmetrically inserted into pGEM3zf(−) (Promega) as described (*8*). One microgram of the double-stranded DNA template was sequenced in both forward (M13-21 universal and KK40 nt 6953 to 6972, 5′-ACAGTACAATGTACACATGG-3′) and reverse [M13 reverse and KK8 nt 6892 to 6917, 5′-AATTTCCCTC(C/T)ACAATTAAAACTGT-3′] directions with the use of dideoxynucleotide triphosphates (Dye-Deoxy terminators) and analyzed with a 373A sequencing system (Applied BioSystems) as described (*8*).
12. S. M. Wolinsky *et al.*, data not shown.
13. The multiple aligned sequence editor (MASE) program [D. Faulkner and J. Jurka, *Trends Biochem. Sci.* **13**, 321 (1988)] was used for the sequence alignments. For phylogenetic analysis, positions where gaps were inserted to maintain the alignment were discounted, leaving 590 positions in the 292 taxa. All sequences from this study were included in a single neighbor-joining tree construction. The phylogenetic tree was constructed with the neighbor program in PHYLIP [J. Felsenstein, *Claudistics* **5**, 164 (1989)] based on a Kimura two-parameter distance matrix with a ratio of transitions to transversions of 1.3. All of the within-subject sequence sets clustered together, indicating that there was no cross-contamination of samples. Additionally, representative viral sequences from each subject were compared to the viral sequences deposited in GenBank with BLAST [S. F. Altschul, W. Gish, W. Miller, E. W. Myer, D. J. Lipman, *J. Mol. Biol.* **215**, 403 (1990)]. No nucleotide sequences with greater than 91% similarity were observed, indicating that contamination with a preexisting viral isolate was unlikely [B. T. M. Korber, G. Learn, J. I. Mullins, B. H. Hahn, S. M. Wolinsky, *Nature* **378**, 242 (1995)].
14. The median branch lengths from each subject's ancestral node to all taxa from a given time point were calculated by means of a Kimura two-parameter distance matrix to create a neighbor-joining tree. For this analysis, we used the two time points closest to the last sampling time point available for P1 (month 26) and P2 (month 35) before death. The median branch length to an ancestral node and the interquartile range was as follows: P1.26, 0.013 (0.013 to 0.018); P2.27, 0.012 (0.009 to 0.015); P2.35, 0.010 (0.009 to 0.010); P3.25, 0.022 (0.018 to 0.024); P3.49, 0.034 (0.033 to 0.034); P4.25, 0.009 (0.006 to 0.011); P4.37, 0.026 (0.021 to 0.035); P5.28, 0.018 (0.013 to 0.021); P5.34, 0.019 (0.015 to 0.027); P6.29, 0.014 (0.012 to 0.016); and P6.39, 0.007 (0.004 to 0.009). There is a trend of less divergence in P1 and P2, with median distances of one and a half– to threefold higher in P3, P4, and P6 at roughly comparable time points. Because P5 had a limited input copy number, it is not possible to ascertain whether the low distance values for P5.29 and P5.39 are exceptions to the trend or sampling artifacts.
15. E. L. Delwart, H. W. Sheppard, B. D. Walker, J. Goudsmit, J. I. Mullins, *J. Virol.* **68**, 6672 (1994).
16. The average numbers of synonymous substitutions per potential synonymous site and nonsynonymous substitutions per potential nonsynonymous site relative to the original consensus sequence were calculated [M. Nei and T. Gojobori, *Mol. Biol. Evol.* **2**, 418 (1986)] for each time point for each of the six study subjects. The consensus sequence from the first sampled time point was used as a reference sequence as the best estimate of the viral form at primary infection. The extrapolated best-fit linear slopes were calculated to estimate the rate of substitution and presented as the percent substitution of each type per annum.
17. For P2, the negative rate of synonymous substitutions calculated per year (−0.2% per year) was due to the low number of synonymous substitutions per synonymous site overall and the relatively greater number of synonymous substitutions in viral sequences from an early time point relative to the consensus sequence than that observed for subsequent time points.
18. S. M. Wolinsky, M. Daniels, M. H. Furtado, J. L. Bingham, B. T. M. Korber, in *Neuvieme Colloque Des Cent Gent Gardes*, M. Girard and B. Dodet, Eds. (La Fondation Marcel Mérieux, Marnes-La-Coquette, France, 1994), p. 95; J. Mullins *et al.*, *ibid.*, p. 77; V. V. Lukashov, C. L. Kuiken, J. Goudsmit, *J. Virol.* **69**, 6911 (1995).

19. Pairwise short tandem repeat (STR)–based [S. Henikoff, *New Biol.* **3**, 1148 (1991)] similarity scores were calculated and used as a basis for the phenograms. For a set of sequences representing a diverse panel of peptides used for a peptide-based enzyme-linked immunosorbent assay [A. Pau *et al.*, *AIDS Res. Hum. Retroviruses* **11**, 1369 (1994)], clusters generated by means of phenograms were highly correlated with the serological typing results (B. T. M. Korber, unpublished results).
20. B. T. M. Korber, K. MacInnes, R. F. Smith, G. Myers, *J. Virol.* **68**, 6730 (1994).
21. The entropy, H_i, is defined in terms of the probabilities, Ps, of the different protein forms, s, that can appear at a given time point i (for example, we consider the symbols $s = A, B, C, \ldots$ to represent the protein clusters defined in Fig. 2). H_i is defined as $H_i = -\sum_{s=A,B,C,\ldots} Ps_i \times \log Ps_i$. This measure, also known as the Shannon entropy, is related to the Simpson index that has been used previously to quantify viral sequence variability within time points (*10*), as both are specific forms of Renyi entropies [A. Renyi, *Probability Theory* (North-Holland, Amsterdam, 1970); P. Grassberger, *Phys. Lett.* **A97**, 227 (1983)]. These analyses correlated with the within-time point amino acid Hamming distances, after gap-stripping.
22. The association of low genetic diversity with a rapid rate of progression to AIDS has been replicated and further substantiated by the results from two natural history cohort studies of HIV-1–infected men based on the heteroduplex mobility assay (E. Delwart *et al.*, in preparation; S. Wolinsky, unpublished results) and by the results of a natural history cohort study of children with perinatal HIV-1 infection (S. Ganeshan *et al.*, in preparation).
23. Neutralization studies were conducted by testing an early and a late isolate against a panel of early sera and late sera from each of the six subjects. Consistent with the observation that a neutralizing antibody response develops gradually [J. P. Moore, Y. Cao, D. D. Ho, R. A. Koup, *J. Virol.* **68**, 5142 (1994)], most of the sera obtained from these participants at an earlier time point had little or no neutralizing activity. The geometric mean titer of the reciprocal dilution of early sera needed to neutralize 90% of an autologous or heterologous virus inoculum (no neutralization was arbitrarily set at 0.01) for all six subjects ranged from 0.03 to 0.06. The geometric mean titers of the reciprocal dilution of late sera needed to neutralize 90% of a virus inoculum were 0.03 for P1, 0.2 for P2, 5.6 for P3, 7.9 for P4, 1.8 for P5, and 0.2 for P6. Therefore, we did not observe a clear association between neutralization capability and the rate of progression to disease. Additionally, the viruses isolated early and late from P1 and the virus isolated late from P2 were the only viruses neutralized by early serum and were generally the most easily neutralized viruses isolated. Mean reciprocal titers of 28.5 and 22.6 were observed for early and late viruses isolated from P1, respectively, and 5.3 for a late virus isolated from P2. The viruses isolated from the blood obtained from the other four subjects had mean reciprocal titers ranging from 0.01 to 3.7. Thus, the propagated viruses from rapid progressors P1 and P2 may be intrinsically easier to neutralize.
24. D. P. W. Burns, C. Collignon, R. C. Desrosiers, *J. Virol.* **67**, 4104 (1993).
25. A. J. McMichael and B. D. Walker, *AIDS* **8**, S155 (1994); J. T. Safrit, A. Y. Lee, C. A. Andrews, R. A. Koup, *J. Immunol.* **153**, 3822 (1994); R. P. Johnson, A. Trocha, T. M. Buchanan, B. D. Walker, *J. Virol.* **67**, 438 (1993).
26. I. Couillin *et al.*, *J. Exp. Med.* **180**, 1129 (1994); M. A. Nowak *et al.*, *Nature* **375**, 534 (1995); B. Autran *et al.*, in *Dixième Colloque Des Ceut Gardes*, J.-P. Levy and M. Girard, Eds. (La Fondation Marcel Mérieux, Marnes-La-Coquette, France, 1996), p. 118.
27. To evaluate the biological phenotype of the viruses isolated from each subject, we tested four to six separate first passage virus culture stocks covering the course of infection for their capacity to replicate in primary cultures of normal donor peripheral blood mononuclear cells and monocyte-derived macrophages and for their syncytium-inducing properties in cultures of the established MT-2–transformed T cell line. The isolated viruses were expanded once in normal donor peripheral blood mononuclear cells, and titers were determined for infectivity as described [R. I. Connor, H. Mohri, Y. Cao, D. D. Ho, *J. Virol.* **67**, 1772 (1993)].
28. R. A. M. Fouchier *et al.*, *J. Virol.* **66**, 3183 (1992); F. de Wolf *et al.*, *AIDS Res. Hum. Retroviruses* **10**, 1387 (1994).
29. M. L. Bonyhadi *et al.*, *Nature* **363**, 728 (1993).
30. R. A. Koup *et al.*, in preparation.
31. J. V. Giorgi *et al.*, *J. Acquired Immune Defic. Syndr.* **5**, 904 (1993); F. Miedema *et al.*, *Immunol. Rev.* **140**, 35 (1994); G. Pantaleo *et al.*, *ibid.*, p. 105; C. Rinaldo *et al.*, *J. Virol.* **69**, 5838 (1995); M. R. Klein *et al.*, *J. Exp. Med.* **181**, 1365 (1995).
32. M. Eigen, *Cold Spring Harbor Symp. Quant. Biol.* **52**, 307 (1987); J. J. Holland, J. C. La Torre, D. A. Steinhauer, *Curr. Top. Microbiol. Immunol.* **176**, 1 (1992).
33. M. Eigen and C. K. Biebricker, in *RNA Genetics*, E. Domingo *et al.*, Eds. (CRC, Boca Raton, FL, 1988), vol. 3, p. 211–245.
34. D. A. Steinhauer, J. C. De La Torre, J. J. Holland, *J. Virol.* **63**, 2063 (1989); D. A. Steinhauer, J. C. De La Torre, E. Meier, J. J. Holland, *ibid.*, p. 2072; J. C. De La Torre, E. Wimmer, J. J. Holland, *ibid.* **64**, 664 (1990).
35. S. Wright, in *Evolution and the Genetics of Populations* (Univ. of Chicago Press, 1977), vols. 1 to 4; *Evolution* **36**, 427 (1982).
36. R. Lande, *Proc. Natl. Acad. Sci. U.S.A.* **82**, 7641 (1985); C. M. Neuman, J. E. Cohn, C. Kipnis, *Nature* **315**, 400 (1985).
37. J. M. Coffin, *Science* **267**, 483 (1995).
38. A. M. Munoz *et al.*, *J. Acquired Immune Defic. Syndr.* **8**, 496 (1995).
39. G. Myers *et al.*, Eds., *Human Retroviruses and AIDS Database* (Theoretical Biology, Los Alamos National Laboratory, Los Alamos, NM, 1994).
40. J. Felsenstein, PHYLIP (phylogeny interference package) version 3.5c; Department of Genetics, University of Washington, Seattle, WA, 1993.
41. D. Swoffend, thesis, University of Illinois, Urbana-Champaign, IL (1988).
42. S. Henikoff, *New Biol.* **3**, 1148 (1991).
43. Supported by the National Institute of Allergy and Infectious Diseases under awards AI-32535, AI-45218, AI-35522, and R-1439-94 and by a gift from an anonymous foundation. We thank D. Panicali and G. Mazzara for the vaccinia constructs; J. Bingham, D. McDonald, S. K. Macomber, and A. Ploss for technical assistance; and L. Chow, J. Moore, J. Theiler, A. Haase, J. Phair, G. Myers, and J. Coffin for advice and discussion. Sequences have been submitted to GenBank under accession numbers U35894 to U36185, and alignments are available from the Human Retroviruses and AIDS Database.

6 October 1995; accepted 4 March 1996

Selective Activation of NF-κB by Nerve Growth Factor Through the Neurotrophin Receptor p75

Bruce D. Carter,*† Christian Kaltschmidt,* Barbara Kaltschmidt, Nina Offenhäuser,‡ Renate Böhm-Matthaei, Patrick A. Baeuerle,§ Yves-Alain Barde

Nerve growth factor (NGF), brain-derived neurotrophic factor (BDNF), and neurotrophin-3 (NT-3) selectively bind to distinct members of the Trk family of tyrosine kinase receptors, but all three bind with similar affinities to the neurotrophin receptor p75 ($p75^{NTR}$). The biological significance of neurotrophin binding to $p75^{NTR}$ in cells that also express Trk receptors has been difficult to ascertain. In the absence of TrkA, NGF binding to $p75^{NTR}$ activated the transcription factor nuclear factor kappa B (NF-κB) in rat Schwann cells. This activation was not observed in Schwann cells isolated from mice that lacked $p75^{NTR}$. The effect was selective for NGF; NF-κB was not activated by BDNF or NT-3.

The best established role for neurotrophins, which include NGF, BDNF, NT-3, NT-4/5, and NT-6, is their ability to support the survival and differentiation of neurons. Three tyrosine kinase receptors, referred to as theTrks, are critically involved in mediating these effects (*1*). However, the neurotrophins also interact with another receptor whose function has not been clearly established, $p75^{NTR}$. The Trks exhibit high selectivity for their cognate ligands (TrkA for NGF, TrkB for BDNF and NT-4/5, and TrkC for NT-3), whereas $p75^{NTR}$ binds to all neurotrophins with similar affinity but with different kinetics (*2*). The Trks produce their effects through activation of well-described signaling pathways, including Ras–mitogen-activated protein kinase, phospholipase C–γ, and phosphoinositol-3-OH kinase (*3*). On the other hand, the transduction mechanisms of $p75^{NTR}$ remain largely unknown. Several reports suggest that $p75^{NTR}$ interacts with TrkA to form a high-affinity binding site (*4*) and to regulate TrkA signaling (*5*). However, evidence has also been presented that suggests that $p75^{NTR}$ has an independent function, such as the regulation of apoptosis (*6*) or the migration of Schwann cells (*7*). The underlying transduction mechanisms have yet to be determined. Recently, neurotrophin binding to $p75^{NTR}$ was shown to activate the spingomyelinase

B. D. Carter and Y.-A. Barde, Department of Neurobiochemistry, Max-Planck Institute for Psychiatry, Martinsried, Germany.
C. Kaltschmidt, B. Kaltschmidt, P. A. Baeuerle, Institute for Biochemistry, University of Freiburg, Freiburg, Germany.
N. Offenhäuser and R. Böhm-Mattaei, Department of Neurochemistry, Max-Planck Institute for Psychiatry, Martinsried, Germany.

*These authors contributed equally to this work.
†Present address: Department of Cell Biology and Anatomy, Cornell University Medical College, New York, NY 10021, USA.
‡Present address: European Institute of Oncology, 20141, Milan, Italy.
§Present address: Tularik Incorporated, South San Francisco, CA 94080, USA.